Corrosion behavior of HPT-deformed TiNi alloys in cell culture medium

D. N. Awang Shri, K. Tsuchiya, and A. Yamamoto

Citation: AIP Conference Proceedings **1877**, 030010 (2017); doi: 10.1063/1.4999866
View online: https://doi.org/10.1063/1.4999866
View Table of Contents: http://aip.scitation.org/toc/apc/1877/1
Published by the American Institute of Physics

Articles you may be interested in

Preparation of tin oxide quantum dots
AIP Conference Proceedings **1877**, 030009 (2017); 10.1063/1.4999865

Phases of $LiMn_{1.84}V_{0.06}Ti_{0.1}O_4$ cathode material
AIP Conference Proceedings **1877**, 040004 (2017); 10.1063/1.4999870

Corrosion behavior of HPT-deformed TiNi alloys in cell culture medium

D.N. Awang Shri[1,a)] K. Tsuchiya[2] and A. Yamamoto[3]

[1]*Faculty of Mechanical Engineering, Universiti Malaysia Pahang, 26600, Pahang, Malaysia*
[2]*Structural Materials Unit, National Institute for Materials Science, Tsukuba, Ibaraki 305-0047, Japan*
[3]*Biomaterials Unit, International Center for Material Nanoarchitectonics (WPI-MANA), National Institute for Materials Science, Namiki 1-1, Tsukuba, Ibaraki 305-0044, Japan*

[a)]*Corresponding author: noorfazidah@ump.edu.my*

Abstract. In recent years there are growing interest in fabrication of bulk nanostructured metals and alloys by using severe plastic deformation (SPD) techniques as new alternative in producing bulk nanocrystalline materials. These techniques allows for processing of bulk, fully dense workpiece with ultrafine grains. Metal undergoes SPD processing in certain techniques such as high pressure torsion (HPT), equal-channel angular pressing (ECAP) or multi-directional forging (MDF) are subjected to extensive hydrostatic pressure that may be used to impart a very high strain to the bulk solid without the introduction of any significant change in overall dimension of the sample. The change in the structure (small grain size and high-volume fraction of grain boundaries) of the material may result in the corrosion behavior different from that of the coarse-grained material. Electrochemical measurements were done to understand the corrosion behavior of TiNi alloys before and after HPT deformation. The experiment was carried out using standard three electrode setup (a sample as working electrode; a platinum wire as a counter electrode and a saturated calomel electrode in saturated KCl as a reference electrode) with the surface area of 26.42 mm^2 exposed to the EMEM+10% FBS cell culture medium. The measurements were performed in an incubator with controlled environment at 37 °C and 5% CO_2, simulating the cell culture condition. The potential of the specimen was monitored over 1 hour, and the stabilized potential was used as the open-circuit potential (EOCP). Potentiodynamic curves were scanned in the potential range from −0.5 V to 1.5 V relative to the EOCP, at a rate of 0.5 mV/s. The result of OCP-time measurement done in the cell culture medium shows that the OCP of HPT-deformed samples shifts towards to the more positive rather than that of BHPT samples. The OCP of deformed samples were ennobled to more than +70 mV for Ti-50mol%. The shift of OCP towards the nobler direction indicates the passive nature of native oxides formed on the surface of the samples. The polarization curve, on the other hand, indicates that the HPT deformation was found to shift the passive current to nobler region. The passive region current density is found to be lower than that of the BHPT, suggesting the passive film formed on the surface of HPT-deformed samples is more protective than that of the BHPT sample. This study has shown that nanocrystallization and amorphization induced by severe plastic deformation change the corrosion behavior of TiNi alloys.

Keywords: Nickel Titanium, Nanocrystalline, Severe plastic deformation, Electrochemical test, Corrosion

INTRODUCTION

Biocompatibility of a metal heavily depends on its corrosion resistance. Corrosion of a TiNi implant is highly concern because of the Ni ion release that has negative effect on the surrounding tissue, inducing allergic response. Toxicity and allergy occur in vivo is related to the corroded metallic materials by body fluids. The failures of implants also might happen as a result of corrosion.

Metallic material have the tendency to corrode in physiological environment thereby accelerating the release of toxic Ni release from TiNi alloys. On the study of surface modification being proven to reduce the Ni ion release, it

4th International Conference on the Advancement of Materials and Nanotechnology (ICAMN IV 2016)
AIP Conf. Proc. 1877, 030010-1–030010-6; doi: 10.1063/1.4999866
Published by AIP Publishing. 978-0-7354-1557-7/$30.00

has been established that the uniformity, not thickness, of the passive oxide layer is more important to prevent TiNi from corrosion [1,2]. HPT deformation produced nanostructured materials consists of nanograins and amorphous region. The change in the structure (small grain size and high-volume fraction of grain boundaries) of the material may result in the corrosion behavior different from that of the coarse-grained material. Although TiNi has a good corrosion resistance due to the protective passive film which primarily composed of TiO_2, the change in the microstructure may influence the corrosion behavior of TiNi.

Potentiodynamic test under physiological fluid provides a fast overview in determining the general corrosion behavior of biometallic material [3]. As most biometal are comprises of passivating alloy, the corrosion behavior of the alloy can be predicted based on its polarization curve.

In this research, the focus is on the electrochemical behavior of TiNi alloys when exposed to the cell culture medium. Electrochemical measurements were done to understand the corrosion behavior of TiNi alloys before and after HPT deformation. The changes in corrosion resistance of the samples and the changes in passive behavior are discussed.

EXPERIMENTAL METHODS

Material Preparations

Ti-50 mol%Ni with analyzed composition of the ingots of Ti-49.8 mol%Ni was used in this experiment. The oxygen content was less than 400 ppm. An ingot was produced by cold-crucible levitation melting. The ingot was forged and hot- and cold-rolled into a plate of about 1 mm thickness. Disk samples with 10 mm in diameter were cut from the plate using a wire electric discharge machine. The disks were heat-treated at 900 °C for 1 hour in vacuum and then water quenched at room temperature. They were then ground to a thickness of 0.85 mm. The disks were then subjected to deformation by high-pressure torsion apparatus (REP-HPT-60-05, Riken Enterprise Co. Ltd) under compressive pressure of 5 GPa at room temperature to various number of rotations, N = 0.25, 0.5, 1, 5 and 10 at a rotation speed of 1 rpm. The deformed samples were then mechanically polished on wet metallographic polishing silicon carbide (SiC) papers consecutively from #220 down to #1000, and then finished with 9-, 3-, and 1- μm diamond paste in order to obtain a mirror-like surface. The polished samples were then cleaned ultrasonically for 15 minutes in acetone.

Electrochemical studies

Electrochemical measurements was carried out using standard three electrode setup (a sample as working electrode; a platinum wire as a counter electrode and a silver/silver chloride in saturated KCl as a reference electrode with the surface area of 26.42 mm^2 exposed to the EMEM+10% FBS cell culture medium. The measurements were performed in an incubator with controlled environment at 37°C and 5% CO_2, simulating the cell culture incubation condition. The potential of the specimen was monitored over 1 hour, and the stabilized potential was used as the open-circuit potential (E_{OCP}). Potentiodynamic curves were scanned in the potential range from −0.5 V to 1.5 V relative to the E_{OCP}, at a rate of 0.5 mV/s. The recording of the current density were done using a VersaSTAT potentiostat, with running VersaStudio software (Princeton Applied Research). Potentiodynamic polarization plots were used to calculate the corrosion potential (E_{corr}) and corrosion current density (i_{corr}) for all the samples using the Tafel extrapolation method. Other corrosion parameter relating to the passive behavior of the samples such as passive current density (i_{pass}), primary passive potential (E_p), and the critical current density (i_c) at E_p can be extracted from the curve.

RESULTS AND DISCUSSION

OCP Measurement and Polarization Curve

The result of OCP-time measurement done in the cell culture medium is shown in Fig. 1. It can be seen that for alloys, the OCP of HPT-deformed samples shifts towards to the more positive rather than that of BHPT samples. In

Ti-50 mol%Ni, the BHPT sample shows some decrease in OCP measurement before finally stabilized at around 750 s, indicating active dissolution of the passive film in cell culture media. The HPT deformed samples, on the other hand, stabilized almost immediately upon immersion. The OCP of deformed Ti-50 mol%Ni samples were ennobled to more than +70 mV. In Ti-50 mol%Ni, the OCP of BHPT sample decreases before stabilized after 800 s. The observed decrease in OCP may be due to the attenuation of the air-formed passive film upon immersion in cell culture medium. On the other hand, the OCP of N=1 and N=5 samples shows some increase in potential before stabilized indicating the formation and growth of further passive film upon immersion in cell culture medium. The other HPT-deformed samples stabilized almost immediately. The shift of OCP towards the nobler direction indicates the passive nature of native oxides formed on the surface of the samples.

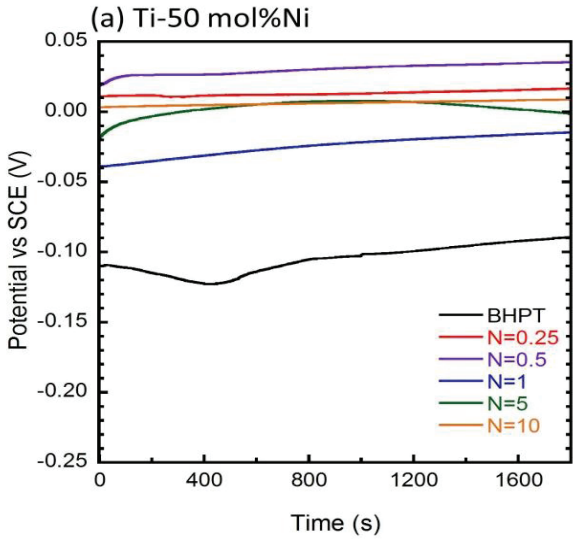

FIGURE 1. Open circuit potential of Ti-50 mol%Ni in cell culture media.

The potentiodynamic polarization curves are shown in Fig.2. All samples show the typical passive behavior. HPT-deformed samples of both TiNi alloys have a nobler corrosion potential (E_{corr}) and a lower corrosion current (i_{corr}) than BHPT samples. These results suggest that the corrosion resistance of TiNi alloys is improved after HPT deformation. Several important parameters, such as steady state passive current density (i_{SS}) and the breakdown potential (E_{bd}) are extracted from the curve and shown in Table 1. The steady state passive current density is marks as i_{ss} while the potential at which the passive film starts to breakdown is denoted as E_{bd}.

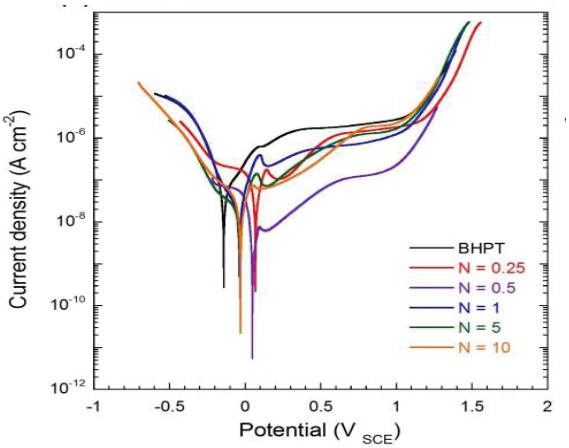

FIGURE 2. The potentiodynamic polarization of Ti-50mol%Ni in cell culture media.

For Ti-50 mol%Ni, a current plateau established spontaneously in the BHPT samples at around 0.1 V indicating the presence of passive region in the solution. The i_{ss} of BHPT was found to be the highest. The HPT deformation

was found to shift down the i_{ss} to nobler region. In the HPT-deformed samples, more pronounced anodic peak corresponds to the start of active-passive transition was observed. The passive range in the deformed samples were slightly inclined until it reached constant between 0.6-0.8 V indicating further passive film formation in the cell culture medium. The passive region current density is found to be lower than that of the BHPT, suggesting the passive film formed on the surface of HPT-deformed samples is more protective than that of the BHPT sample. A sudden increase in current density around 1-1.2 V denotes the breakdown of the passive range and the initiation of localized pitting corrosion. However, the pitting potential of all samples are almost identical, suggesting that the pitting resistance of TiNi does not change after HPT deformation. Nonetheless, the pitting potential occur more than 1 V from open circuit potential, suggesting that the spontaneous pitting corrosion will not happen in the cell culture medium.

TABLE 1. Corrosion parameter of Ti-50 mol%Ni

	OCP (mV)	E_{corr}(mV)	I_{corr} (nA·cm^2)	I_{ss}(nA·cm^2)	E_{bd}(V)
BHPT	-73.92	-139.84	71.23	1638.24	1.07
N=0.25	22.08	68.95	50.76	1275.58	1.14
N=0.5	40.79	48.63	5.16	418.96	0.95
N=1	-8.59	-40.69	21.31	518.99	1.03
N=5	-26.38	-36.15	13.84	927.55	1.04
N=10	83.42	-29.99	46.07	1593.43	1.00

Nanocrystallization and amorphization induced by severe plastic deformation is shown to change the corrosion behavior of TiNi alloys. Investigation on open circuit potential reveals HPT deformation shift the OCP of TiNi sample to more positive value in comparison to BHPT samples in both TiNi alloys. The shift towards more noble potential indicates the passive film formed prior immersion in the cell culture medium is more protective. The OCP for HPT samples also stabilized immediately or increase to higher potential signaling the stability of the passive film.

The results of potentiodynamic test revealed that the samples after HPT deformation have more stable and protective oxide film on the surface. In comparison to the HPT deformed samples, higher passive current density as observed in the BHPT samples in both alloys indicates the defective nature of the passive film [4]. Slight incline in the beginning of the passive range in the HPT deformed samples indicates the passive film still continues to increase before finally reaching stable state.

Passive film formed on TiNi alloys serve as strong barriers between TiNi alloys and the physiological environment. However, after subjected to HPT deformation, the amount and composition of the passive films varies depending on the HPT rotations. Although in general thicker passive films improve the corrosion rate, the thickness is not the only factor influencing corrosion behavior of an alloy. Other factors, such as oxide structure, adherence to the substrate, presence of defect and chemical composition, also play role in determining the corrosion rate. The uniformity and stability of the oxide is most important to protect the materials from corrosion [1]. Few works has been done in investigating the effect of nanocrystallization and amorphization on the corrosion resistance of TiNi. Amorphous TiNi alloys prepared by melt spinning also shows improvement in corrosion resistance. Mathur et. al. attributed the corrosion resistance of amorphous TiNi alloys are due to the different oxide species on the surface oxide [5]. Recently, the effect of SPD process on the corrosion behavior of TiNi was also examined. Early work by Trepanier et. al. has shown that straining up to 10% did not affect the corrosion resistance of TiNi alloys [6]. Tuschiya et. al. reported that corrosion current density of Ti-50.9 mol%Ni in 1M HNO_3 decreases after shot-peened with Fe-C at 0.6 MPa even though the surface area increases due to surface roughness[7]. Electrochemical investigation using physiological fluid on nanocrystalline TiNi alloys also has been reported. Amorphous and nanocrystalline Ti-50.2 mol%Ni fabricated via HPT deformation process has been subjected to corrosion test in artificial saliva and Hank's solution by Nie et. al. [8]. Another works by Hu et.al. also shows corrosion resistance of Ti-50.8mol%Ni in 0.9% NaCl physiological fluid was enhanced after SMAT process due to readily protective formed passive film on the surface [9]. The enhanced corrosion resistance on other SPD-deformed passive alloys such as titanium and stainless steel also has been reported. Ultrafine grained Ti produced by ECAP had better corrosion resistance than coarse grain Ti in HCl and H_2SO_4 solutions [10]. Nanocrystalline 302 stainless steel

prepared by ECAP also shows better corrosion resistance due to improved in compactness and stability of the passive films [11].

The structural changes induced in TiNi alloys after HPT deformation allows the formation of more uniform passive film [12]. The stability of the passive film depends on the structural properties such as film compactness and defect density [13]. Improved corrosion resistance of TiNi as observed in this study may be attributed to the nanocrystallization and amorphization induced by HPT deformation. Enhance corrosion resistance of nanostructured alloys is attributed to the high density of grain boundaries that provides fast diffusion paths [13]. As the corrosion activation occurs primarily at the surface defects, such as grain boundaries and dislocations, small grain sizes promote uniform Ni and Ti distribution, which facilitates rapid formation of oxide layer. High densities of dislocation and grain boundary cause the drive to achieve energy equilibrium state through fast passivation and homogeneous corrosion [10]. The higher energies stored in the non-equilibrium grain boundaries and high internal stress generated during HPT resulting in formation of uniform passive film [14]. Dislocations created during deformation reduced the energy barrier for electrochemical reactions. Nanocrystallization was found to change the surface condition of the alloys, but also effectively increase the activity of metallic atoms and accelerate the corrosion rate [15]. The activation barrier to dissolution from nanocrystalline Ni surfaces is higher compared to bulk Ni, thereby resulting in improved corrosion resistance for nanostructured surfaces compared to bulk surfaces. This may be related to the observation that nanocrystalline Ni showed lower tendency for localized grain boundary corrosion while in polycrystalline Ni, this can result in failures [4].

CONCLUSION

The effect of HPT deformation on electrochemical behavior of TiNi alloys has been compared in this chapter. The shift in OCP to the more positive potential in HPT deformed samples indicates the ennoblement of the samples surface upon immersion in cell culture medium. The passive current density of the HPT deformed samples also were found to be lower in comparison to the BHPT sample in both alloys, indicating the passive film formed is more protective. This study concluded the beneficial effects of HPT deformation on the corrosion resistance of TiNi alloys in the cell culture medium due to formation of more stable and protective passive film on the TiNi alloys after HPT deformation.

ACKNOWLEDGEMENTS

This work is partly supported by the Grant-in-Aid for Scientific Research on Innovative Area, “Bulk Nanostructured Metals”, through MEXT, Japan (contract No. 22102004). One of the authors (DNAS) also would like to acknowledge the support from University Malaysia Pahang, Malaysia (RDU150385).

REFERENCES

1. Duerig T, et al. An overview of nitinol medical applications. Mater. Sci. Eng. A **273**, 149 (1999).
2. Vojtěch D, et al. Surface treatment of NiTi shape memory alloy and its influence on corrosion behavior. Surf. Coat. Tech. **204** 3895, (2010).
3. Pourbaix M. Electrochemical corrosion of metallic biomaterials. Biomaterials **5** , 122 (1984).
4. Mishra R, et al. Effect of nanocrystalline grain size on the electrochemical and corrosion behavior of nickel. Corros. Sci.;**46**, 3019, (2004).
5. Mathur S, et al. XPS characterization of corrosion films formed on the crystalline, amorphous and nanocrystalline states of the alloy Ti60Ni40. J Non Cryst Solids **357**, 1632 (2011).
6. Trepanier C, et al. Effect of strain on the corrosion resistance of nitinol and stainless steel in simulated physiological environment. Medical Device Materials: Proceedings From the Materials & Processes for Medical Devices Conference 2003, 8-10 September 2003, Anaheim, California:**176** (2004).
7. Tsuchiya K, et al. Nanostructured Shape Memory Alloys for Biomedical Applications. Mater. Sci. Forum;**539-543**, 505 (2007).
8. Nie FL, et al.. In vitro corrosion and cytotoxicity on microcrystalline, nanocrystalline and amorphous NiTi alloy fabricated by high pressure torsion. Mater. Lett.;**64**, 983 (2010).
9. Hu T, et al.. Corrosion behavior on orthopedic NiTi alloy with nanocrystalline/amorphous surface. Mater. Chem. Phys.;**126**, 102 (2011).

10. Balyanov, A., et al. "Corrosion resistance of ultra fine-grained Ti." Scripta Materialia **51.3**, 225 (2004).
11. Zheng, Z. J., et al. "Corrosion behaviour of nanocrystalline 304 stainless steel prepared by equal channel angular pressing." Corrosion Science **54**, 60 (2012).
12. Awang Shri, D.N., et al. "Surface characterization of TiNi deformed by high-pressure torsion." App. Surf. Sci. **289,** 338 (2014).
13. Wang Y, et al. Electrochemical behaviour of Fe-based metallic glasses in acidic and neutral solutions. Corros. Sci.;**63**, 159 (2012).
14. Saji VS, et al.Nanomaterials for corrosion control. Curr Sci, **92**, 51 (2007).
15. Dolega Ł, et al.Corrosion resistance of model ultrafine-grained Al–Li alloys produced by severe plastic deformation. J Mater Sci. **47**, 3026 (2011).
16. Liu L, et al. Electrochemical corrosion behavior of nanocrystalline materials-a review. J. Mater. Process. Tech. **26**, 1 (2010).